Fırat Üniversitesi Müh. Bil. Dergisi
38(1), 381-393, 2026

*Araştırma Makalesi*
https://doi.org/10.35234/fumbd.1831874

# Aluminum Recovery and Process Optimization from High-Silica Kemiklitepe (Türkiye) Bauxite Ore by the Alkaline Roasting-Water Leaching Method

**Turan UYSAL**[1*]
[1]Department of Mining Engineering, Faculty of Engineering and Natural Sciences, Gümüşhane University, Gümüşhane
[*1] turanuysal@gumushane.edu.tr

**(Geliş/Received: 28/11/2026; Kabul/Accepted: 10/03/2026)**

**Abstract:** In this study, an innovative and environmentally friendly alternative method was investigated for aluminum recovery from diasporic bauxite, classified as a critical raw material, without using caustic soda. Within this context, the alkaline roasting–water leaching combination was applied to enhance aluminum recovery from high-silica bauxite ore. Optimization of the process parameters was carried out using Response Surface Methodology (RSM). The effects of key parameters, roasting temperature, milling time, and ball-to-powder/ore ratio (BPR), on Aluminum (Al) dissolution were systematically evaluated through the RSM design. The reliability of the model was confirmed by ANOVA analysis, and the regression results indicated that the coefficient of determination ($R^2$) exceeded 90% for all responses, demonstrating a strong model fit. According to the optimization outcomes, the optimum conditions were determined as a roasting temperature of 919 °C, a milling time of 90 minutes, and a BPR of 23. Water leaching results revealed that aluminum recovery increased by approximately 26% in the ore roasted at 1000 °C compared to the raw (unroasted) ore. Overall, the findings indicate that the alkaline roasting–water leaching method is a promising alternative for processing high-silica bauxite deposits.

**Keywords:** Bauxite, intensive milling, alkaline roasting, leaching, optimization, aluminum.

# Yüksek Silisli Kemiklitepe (Türkiye) Boksit Cevherinden Alkali Kavurma-Su Liçi Yöntemiyle Alüminyum Kazanımı ve Proses Optimizasyonu

**Öz:** Bu çalışmada, kritik bir hammadde olarak sınıflandırılan diasporik boksitten kostik soda kullanılmadan Al kazanımı için yenilikçi ve çevre dostu alternatif bir yöntem araştırılmıştır. Bu kapsamda yüksek silis içerikli boksit cevherinden alüminyum kazanımını artırmak amacıyla alkali kavurma–su liçi kombinasyonu uygulanmıştır. Proses parametrelerinin optimizasyonu ise Yanıt Yüzey Metodu (RSM) kullanılarak gerçekleştirilmiştir. Kavurma sıcaklığı, öğütme süresi ve BPR gibi temel parametrelerin Al çözünürlüğü üzerindeki etkileri, RSM tasarımı ile sistematik olarak değerlendirilmiştir. Modelin güvenilirliği ANOVA analizleriyle doğrulanmıştır. Regresyon analizleri, tüm yanıtlar için determinizasyon katsayısının ($R^2$) %90'ın üzerinde gerçekleştiği ve model uyumunun yüksek olduğu belirlenmiştir. Optimizasyon sonuçlarına göre en uygun parametreler; 919 °C kavurma sıcaklığı, 90 dakika öğütme süresi ve 23 BPR olarak belirlenmiştir. Su liçi sonuçlarına göre, kavrulmamış cevhere kıyasla 1000 °C'de alkali kavrulan cevherde Al kazanımının yaklaşık %26 oranında arttığını ortaya koymuştur. Bulgular, yüksek silis içerikli boksitlerde alkali kavurma-su liçi yönteminin umut vaat eden alternatif bir yöntem olarak değerlendirilebilir. Ayrıca sonuçlar, prosesin endüstriyel ölçekte uygulanabilirliğine yönelik önemli bir potansiyel sunduğunu ortaya koymaktadır.

**Anahtar kelimeler:** Boksit, aşırı öğütme, alkali kavurma, liç, optimizasyon, alüminyum.

## 1. Introduction

For metallurgical-grade bauxites, the mass ratio between alumina ($Al_2O_3$) and reactive silica ($SiO_2$), known as the silica modulus, is of critical importance for the Bayer process. Reactive silica forms insoluble sodium aluminosilicate hydrate, referred to as desilication product, which causes significant losses of both alumina and caustic soda. Therefore, for the Bayer process to remain economically viable, the silica modulus of the feed bauxite must be maintained at an optimum level. Although the optimum value varies depending on the bauxite type and techno-economic conditions of the plant, the lower limit is generally accepted to be around 7-8. High-quality bauxites typically exhibit a modulus value above 10 [1-2]. However, bauxite deposits with such high grades are limited in number, and their reserves are steadily decreasing. In contrast, low-modulus bauxites are more widely distributed and possess larger reserves, yet their high silica content prevents their direct use in the Bayer process. Many methods have been developed to obtain alumina from high-silica bauxite. Most of these methods are still at the experimental stage, and only a few have been industrially implemented. The flotation–Bayer process has been

[*] Sorumlu yazar: turanuysal@gumushane.edu.tr Yazarların ORCID Numarası: 0000-0003-1643-6725

widely applied in alumina refineries; however, it involves large quantities of hazardous organic reagents and generates waste equivalent to approximately 25 wt% of the initial bauxite ore. The lime-Bayer process has also been used to treat certain portions of high-silica bauxites, but it cannot economically process ores with a silica modulus below 5 [3]. For high-silica bauxites with a silica modulus lower than 5, combinations of the lime-soda sintering process and the Bayer process are preferred [4]. Nevertheless, due to the high operating costs, these methods are not economically feasible. In other words, there is still no industrial method that can process high-silica ores in an economically and environmentally viable manner.

To address the challenges associated with the high silica content of bauxites, various methods have been proposed. Nevertheless, technological and economic limitations have prevented these approaches from fully resolving the silica issue. As a result, the efficient utilization of high-silica bauxite has become an urgent and significant challenge for the alumina industry [5]. While alkaline methods hold a prominent position in alumina production, acid-based methods offer advantages such as minimizing and recycling bauxite residues. For this reason, Sun et al. [5] attempted to combine alkaline and acid approaches to achieve zero-waste extraction of $Al_2O_3$ and $SiO_2$ from high-silica bauxite. In their study, the ore was first activated by sintering with $Na_2CO_3$, followed by water leaching to obtain a sodium aluminate solution. The insoluble residue from water leaching was subsequently subjected to sulfuric acid leaching to transfer $SiO_2$ and the remaining $Al_2O_3$ into the pregnant solution. Silica gel and polyaluminum ferric sulfate were then produced via polymerization of this solution. Similarly, Valeev et al. [6] investigated a boehmitic bauxite from Severoonezhsk (Russia), characterized by a high silica content ($\mu_{Si}< 3$), rendering it unsuitable for processing via the Bayer route. They applied a bisulfate method ($H_2SO_4$ and $NH_4SO_4$), combining advantages of both acid and alkaline processes. The effects of leaching temperature (130-200 °C), solution-to-ore ratio (8-12), and leaching time (5-90 min) on Al and REE dissolution were examined. Dissolution efficiencies for Al, Fe, and Ga exceeded 90%, whereas most silica and titanium remained in the solid residue. Togacar et al. [7] employed sodium carbonate-assisted roasting followed by water leaching and crystallization for the valorization of diasporic bauxite. The proposed method enabled the formation of water-soluble sodium aluminate phases at relatively moderate temperatures (1000 - 1100 °C), achieving high alumina recovery. In the optimized process, $Al(OH)_3$ containing 62.20 wt.% $Al_2O_3$ was produced, which was subsequently calcined to obtain alumina with 97.30% purity. Li et al. [8] proposed a novel zero-waste process involving pre-roasting followed by two-stage leaching. When the roasting temperature exceeded 310 °C, diaspore and kaolinite lost their structural water, gradually transforming into alumina and metakaolin, respectively. At temperatures above 950 °C, metakaolin decomposed into an amorphous aluminosilicate phase and silica. Increasing the roasting temperature and duration enhanced the crystallinity of the resulting alumina and silica phases, thereby reducing the leaching efficiency. Optimal roasting conditions were identified as 1050 °C for 30 min, yielding Al and Si leaching efficiencies of over 94% and 88%, respectively.

Although the Bayer process remains the principal method for alumina and aluminum production from bauxite, countries with limited bauxite resources or those lacking ores suitable for the Bayer route depend heavily on imports. Additionally, the mandatory disposal of red mud generated during the Bayer process poses environmental risks, further motivating the search for alternative aluminum sources [9-10]. Even countries with sufficient bauxite reserves are actively exploring alternative production routes to reduce energy consumption or produce alumina and aluminum from non-bauxite resources with lower energy input [11-13]. Consequently, many countries have turned their attention to producing aluminum from high-silica bauxite deposits.

Mechanical activation is defined as an “increase” in the reactivity of a solid that remains chemically unchanged during the milling process in which mechanical energy is transferred. During mechanical activation, while the particle size of the mineral decreases due to milling, defects are introduced into the crystal structure depending on the intensity of mechanical energy [14]. This results in the formation of fresh, clean surfaces and metastable species [15]. The mechanical activation of minerals enhances the selectivity of dissolution and the effectiveness of the solvent during leaching, leading to an increase in reaction rate [16]. This enhancement arises from the increase in specific surface area and structural disorder, the development of microstrains [17], amorphization of mineral crystals [18], microtopographic changes [19], formation of new phases more prone to dissolution [20], and increased susceptibility to thermal reduction [21]. Under conditions of mechanical activation, the mineral behaves more actively during subsequent metallurgical processes, such as calcination [22], roasting [23], or leaching [24], which can result in either a reduction of process temperature or an increase in reaction rate.

In this study, the recoverability of aluminum from bauxite ores with elevated silica content unsuitable for direct processing by the Bayer method was investigated. For this purpose, the Kemiklitepe bauxite ore was evaluated within the context of sustainable resource utilization using water and acid leaching. Specifically, the high-silica bauxite sample was subjected to an alkaline roasting-water leaching process, and the optimization of the process parameters was carried out using RSM.

## 2. Materials and Methods
### 2.1. Materials

The bauxite ore used in this study was obtained from deposits located in the Karaman-Ayrancı region. A representative sample was collected from the crushing-screening facility situated in the Toroslar district of Mersin Province. The mineralogical composition of the Kemiklitepe bauxite ore was determined by XRD analysis and is presented in Figure 1. The ICP-AES analysis results of the bauxite ore are given in Table 1.

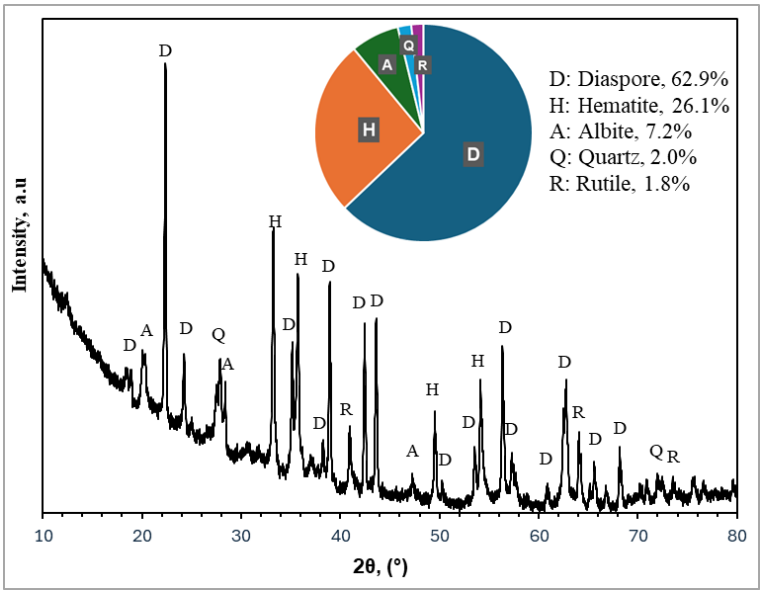


**Figure 1.** XRD pattern of Kemiklitepe bauxite ore

According to Figure 1, the main minerals present in the ore are diaspore (α-AlOOH), hematite ($Fe_2O_3$), quartz ($SiO_2$), albite ($NaAlSi_3O_8$), and rutile ($TiO_2$). Based on the results of the mineralogical analysis, it is understood that the sources of $Al_2O_3$ are diaspore and albite, while the sources of $SiO_2$ are albite and quartz. $TiO_2$ is derived from anatase, and $Na_2O$ originates from albite. Additionally, the presence of $Fe_2O_3$ in the ore is attributed to hematite.

**Table 1.** Chemical composition of Kemiklitepe bauxite ore determined by ICP-AES, wt%

| $SiO_2$ | $Al_2O_3$ | $Fe_2O_3$ | CaO | MgO | $Na_2O$ | $K_2O$ | $TiO_2$ | MnO | $P_2O_5$ | LOI |
|---|---|---|---|---|---|---|---|---|---|---|
| 15.6 | 47.8 | 22.4 | 0.40 | 0.06 | 1.50 | 0.63 | 2.43 | 0.06 | 0.10 | 9.62 |

Table 1 shows that the silica modulus of the ore ($Al_2O_3/SiO_2$: 3.06) is not suitable for the Bayer process, indicating a high silica content.

Within the scope of this study, the ore was characterized using the following instrumental analysis methods. X-ray diffraction (XRD) analysis was employed to determine the mineral composition of the raw bauxite ore and roasted products, as well as to monitor changes in the crystal properties of these minerals due to roasting. XRD patterns were obtained using an XRD device (Karadeniz Technical University) with CuKα radiation, a scanning rate of 2°/min, and diffraction angles ranging from 5° to 80°. Mineral identification was carried out using the Powder Diffraction File (ICDD-PDF) database provided with the instrument by The International Centre for Diffraction Data. Quantitative analysis of the ore based on XRD data was performed using the Rietveld method. To determine the chemical composition of the ore samples, ICP-MS and ICP-AES instruments (Perkin Elmer Elan 9000, ALS Labs Galway, Ireland) were used. The particle size distribution of the milled ore was measured using a Malvern Mastersizer 2000 (Karadeniz Technical University, Department of Mining Engineering). Scanning Electron Microscopy (SEM, Hitachi SU3500, Japan) was employed to examine the micromorphological properties of the samples.

## 2.2. Methods

### 2.2.1. Intensive milling

The representative coarse bauxite sample obtained from the crushing-screening plant was milled to a particle size of -212 µm. The −212 µm particle size was selected as an appropriate compromise by taking into account the balance between leaching efficiency and milling-related energy consumption. The milled material was subsequently sieved using ASTM E-11 standard test sieves and homogenized by dividing it into representative with a rotary sample splitter.

To achieve mechanical activation of the ore, intensive milling was performed using a vibratory ball mill (Ünal brand). The milling process was conducted in an energy-efficient, air-cooled vibratory mill equipped with a 100 cm³ tungsten carbide milling vessel and 10 mm diameter tungsten carbide balls of the same composition. Prior to milling, all samples were dried at 105 °C for at least 1 hour to remove surface moisture and then allowed to cool in a desiccator.

### 2.2.2. Alkaline roasting

The alkaline roasting process allows for a reduction in sintering temperature, thereby decreasing energy consumption. $Na_2CO_3$ is a highly economical material and is widely used in industry. To enhance the solubility of the ore, bauxite samples were homogeneously mixed with $Na_2CO_3$ prior to alkaline roasting. The dosages of additives are generally determined based on the contents of the main components in the bauxite. In the conventional lime-soda process, the dosages of $Na_2CO_3$ and CaO are controlled at molar ratios of $Na_2O/Al_2O_3$: 1 and $CaO/SiO_2$: 2, respectively, to promote the formation of $NaAlO_2$ and $Ca_2SiO_4$ [3]. In this study, since CaO is absent, both $Al_2O_3$ and $SiO_2$ will react with $Na_2CO_3$. Therefore, the molar ratio of $Na_2O/(Al_2O_3 + SiO_2)$ was used as an indicator to control the $Na_2CO_3$ dosage. The mixture was prepared at a molar ratio of $Na_2O/(Al_2O_3 + SiO_2)$: 1, based on previously published studies [5].

The roasting process was carried out in a chamber furnace, capable of reaching a maximum temperature of 1200 °C, under non-isothermal conditions in an air atmosphere. The samples were heated at 800, 900, 950, and 1000 °C for 30 minutes. The heating rate of the furnace was kept constant at 20 °C/min.

### 2.2.3. Water leaching

The leaching experiments were carried out in a vacuum oven using a setup consisting of a 500 cm³ jacketed flask equipped with a magnetic stirrer, under a reflux condenser, with continuous monitoring of the solution temperature. Upon completion of the leaching period, the heating and stirring systems were immediately stopped, and the solid-liquid separation was performed using vacuum filtration. The volume of the resulting filtrate was recorded after washing, and the solution was transferred into capped plastic containers and stored in a refrigerated cabinet.

### 2.2.4. Experimental design and optimization

In this study, three independent variables, roasting temperature, milling time, and ball-to-ore ratio, were optimized using the RSM. The effects of these parameters on leaching recovery were investigated using a central composite design, and mathematical models were developed. This method allows for experimental work and replication, excluding the center points. Using this design, the variations and interactions of all variables can be examined within the same process. Statistical analyses were performed using Minitab-22 software. The results were statistically evaluated at a 95% confidence level using ANOVA. Once the response data were obtained from the experiments, regression analysis was conducted to determine the model coefficients, their standard deviations, and magnitudes. The second-order polynomial equation used to describe the dependent variables is given in Eq. 1.

$$Y = \beta_0 + \sum_{i=1}^{k} \beta_i X_i + \sum_{i<j}^{k} \beta_{ij} X_i X_j + \sum_{i=1}^{k} \beta_{ii} X_i^2 + \ldots \quad (1)$$

Here, $y$represents the dependent variable (leaching recovery) as a function of the coded independent variables $x_1$, $x_2$, and $x_3$. $\beta_0$is the regression coefficient, $\varepsilon$is the error term, $\beta_i$are the linear coefficients, $\beta_{ii}$are the quadratic coefficients, and $\beta_{ij}$are the interaction coefficients. The parameters studied for the optimization of bauxite milling and roasting are presented in Table 2.

**Table 2.** Minimum and maximum values of the parameters used in the optimization study

| Parameters | Values |
|---|---|
| Roasting temperature | 700-900 °C |
| Milling time | 0.5-3 h |
| Ball-to-Powder ratio | 7.5-20.0 |
| Leaching recovery | 0-100% |

## 3. Results and Discussion

### 3.1. Intensive milling

The appearances of the ore after milling under different conditions are shown in Figure 2. The particle size distributions of the normally and intensive milled ore are presented in Figure 3.

**3-14** **113-14** **222-14**

**Figure 2.** Mortar appearances after milling under different conditions

As shown in Figure 2, under the milling condition with a milling time of 3 minutes and a ball-to-powder ratio (BPR) of 14 (3-14), slight layering is observed on the mortar walls and the surface of the milling balls. In contrast, under the condition of 113 minutes of milling with the same BPR (113-14), a pronounced crust formation appears on the walls and on the upper layer of the sample. This indicates an increased tendency toward agglomeration under this condition and suggests that prolonged milling may reduce milling efficiency. At 222 minutes of milling, bed formation on the mortar walls is observed, as seen in the image.

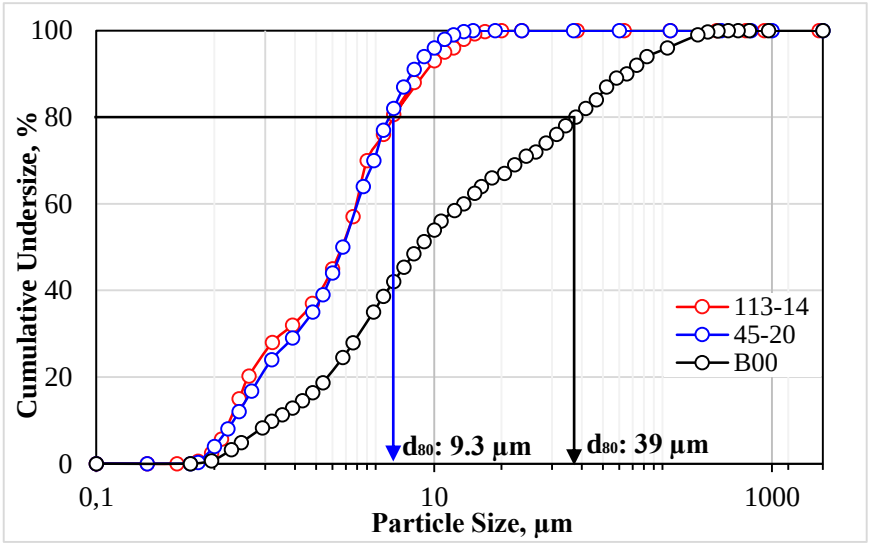


**Figure 3.** Particle size distribution curves of conventional and intensive milled ore

According to the results presented in Figure 3, the $d_{80}$ value of the conventional ground (B00) ore is 39 µm, whereas the $d_{80}$ value of the ore milled for 45 minutes decreases significantly to 9.3 µm. The particle size distribution curves for 45-minute and 113-minute milling are steeper and shifted to the left compared to B00,

indicating that the proportion of fine particles increases as milling time increases. The PSD patterns obtained under the 45-20 and 113-14 milling conditions exhibit similar trends; therefore, the effect of the difference in milling time is considered to be minor. While the normally ground bauxite ore exhibits a relatively coarse and broad particle size distribution, the intensive milled samples show smaller particle sizes with a narrower distribution.

A comparison of the XRD peaks of the intensive milled ore under different conditions is presented in Figure 4. XRD analysis was employed to evaluate the effect of intensive milling on the crystal structures of the mineral phases. With increasing milling time, structural alterations such as decreased peak intensities, peak broadening, and reduced crystallinity are anticipated as typical consequences of mechanical activation.

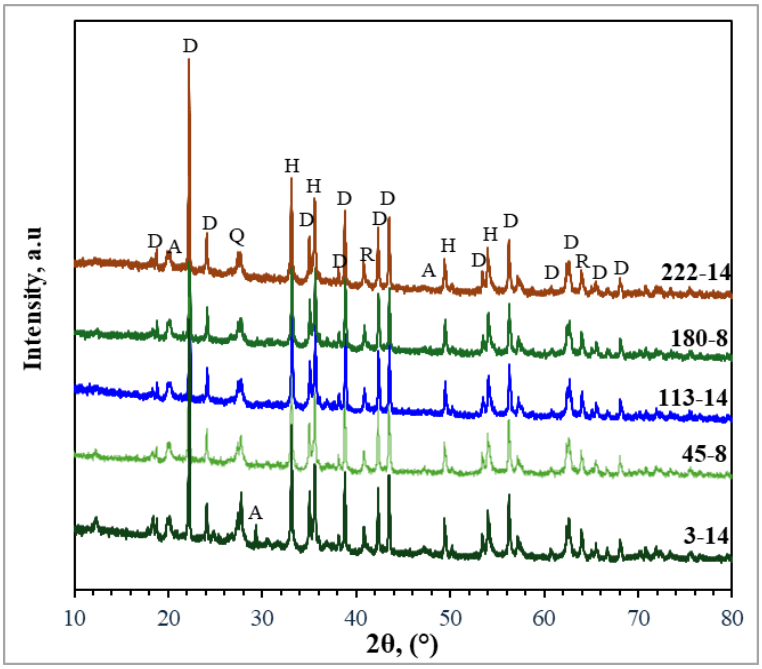


**Figure 4.** Comparison of XRD peaks of unmilled and milled samples under different conditions

Upon examination of the XRD peaks in Figure 4, the albite peaks at 12.75°, 18.72°, 29.8°, and 47.90° disappear as a result of milling. No significant changes are observed in the peaks corresponding to diaspore, hematite, rutile, and quartz. Peak broadening is evident in some peaks of the samples milled for longer durations (222-14), indicating a reduction in crystallite size, the presence of internal strain, and partial amorphization. Samples milled under the 3-14 condition exhibit sharper and narrower peaks, suggesting that their crystal structure remains largely intact. For the 222-14 and 180-8 conditions, certain peak intensities decrease or broaden due to the effects of milling.

### 3.2. Alkaline roasting

The SEM images in Figure 5 were presented to evaluate the microstructural effects of roasting at different temperatures. In the SEM image shown in Figure 5 (0-113-14), a broad particle size distribution is observed for the unroasted ore that is, small particles and aggregates are present together. In the intensively milled samples, the formation of aggregates of various sizes is observed. Figure 5 shows the sample labeled 637-113-14, representing the bauxite ore milled for 113 minutes at a BPR of 14 and subsequently alkaline-roasted at 637 °C. Under these conditions, the particles developed a porous morphology as a result of the combined effects of milling and roasting. Such a structure indicates that the sample becomes more amenable to dissolution during the leaching stage. Following alkaline roasting at 800 °C, the ore exhibited a distinctly agglomerated and more compact surface morphology. In addition, needle-like crystals with a mullite-like character commonly associated with the rearrangement of silica-alumina phases during high-temperature alkaline roasting were also observed in agreement with the literature [25]. After roasting at 963 °C, the SEM image reveals that the ore structure transformed into a sintered and strongly agglomerated morphology. Consequently, the particles fused together, producing a compact,

dense, and low-porosity texture. Compared to the structures formed at lower temperatures, this morphology is expected to be less reactive and to exhibit limited solubility during subsequent leaching.

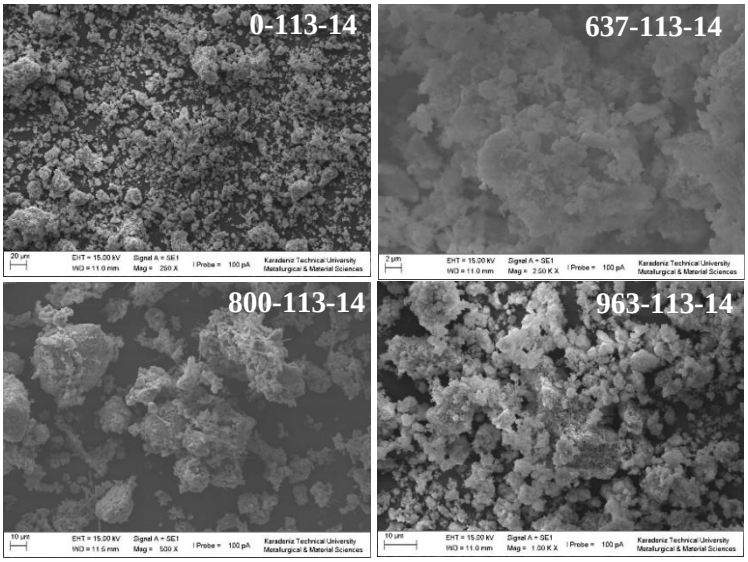


**Figure 5.** SEM images of unmilled and bauxite samples milled under different conditions

In this study, based on relevant literature, the roasting duration was fixed at 30 minutes, while the roasting temperature was varied between 800, 900, 950, and 1000 °C. The appearances of the bauxite ore after alkaline roasting at different temperatures are shown in Figure 6.

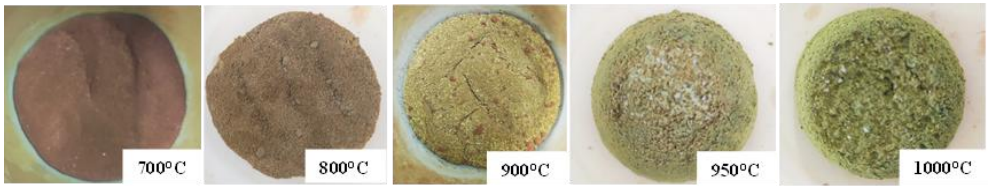


**Figure 6.** Color change of samples after alkaline roasting

The primary reason for the color transition from red to green is the reaction of $Fe_2O_3$ in the bauxite with $Na_2CO_3$, forming sodium ferrite ($NaFeO_2$) and/or greenish-black iron oxide phases such as $Fe_3O_4$ [26]. After alkaline roasting, the samples become hard, consolidated solids due to sintering; therefore, they were ground in an agate mortar prior to water leaching. The following processes occur when bauxite ore and $Na_2CO_3$ are subjected to alkaline roasting at different temperatures. At elevated temperatures, $Na_2CO_3$ reacts with $Fe_2O_3$ to form sodium ferrite ($NaFeO_2$) compounds (Eq. 2).

$$Fe_2O_3 + Na_2CO_3 \longrightarrow 2NaFeO_2 + CO_2 \quad (2)$$

Sodium ferrite ($NaFeO_2$) typically exhibits a greenish-black coloration. Additionally, transformations such as the conversion of hematite (red) to magnetite ($Fe_3O_4$, greenish-black) may occur. These phase changes collectively contribute to the greenish tones observed in the roasted samples. The mass changes of the samples after alkaline roasting are presented in Figure 7. The XRD patterns of the samples roasted at different temperatures are shown in Figure 8.

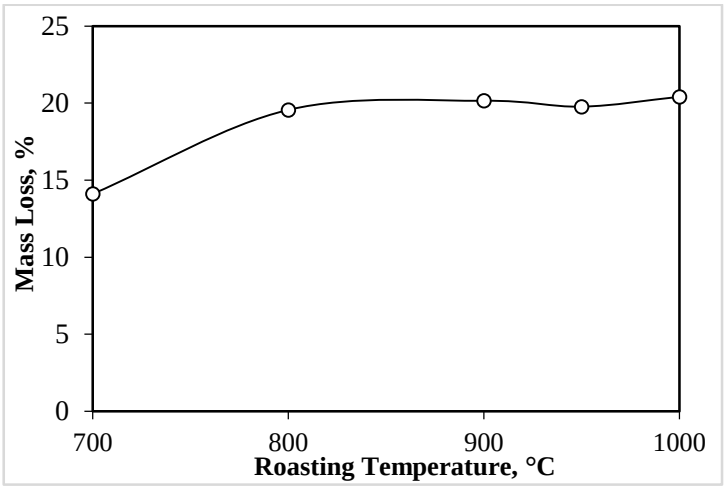


**Figure 7.** Mass loss of bauxite ore after alkaline roasting

In Figure 7, the significant mass loss observed at 700 °C is largely attributed to the dehydroxylation of structural hydroxyl groups. The increase in mass loss between 700-800 °C is likely due to active reactions occurring between the alkaline ($Na_2CO_3$) and the ore, as well as the release of $CO_2$/$H_2O$ gases. Above 800 °C, the curve becomes nearly constant, indicating the depletion of reactive phases.

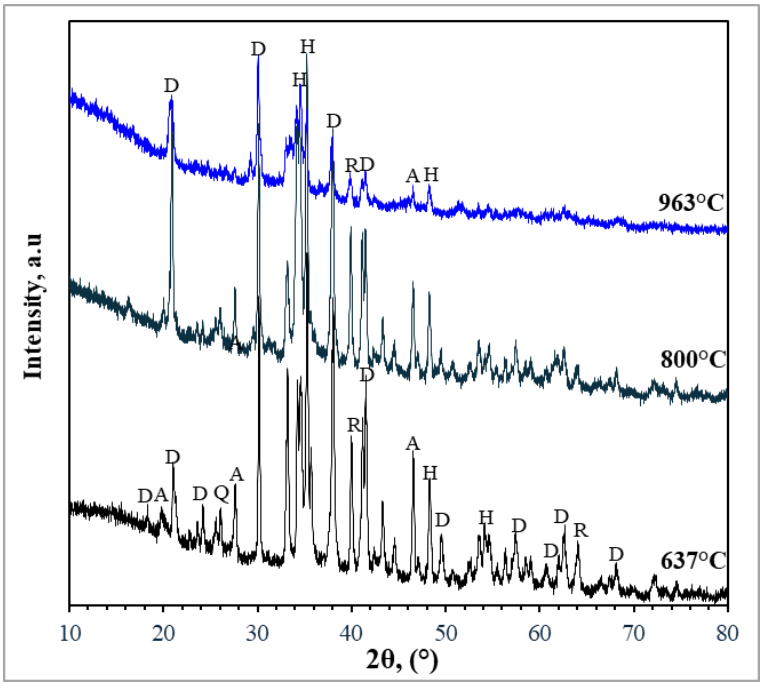


**Figure 8.** XRD patterns of the ore alkaline-roasted at different temperatures

In Figure 8, while the mineral crystal structures remain intact at 637 °C, diaspore begins to decompose at 800 °C, initiating the formation of γ-$Al_2O_3$ and leading to the deterioration of the crystalline framework. At 963 °C, diaspore disappears completely, leaving $Al_2O_3$ and hematite as the stable phases, whereas quartz becomes weakened and partially transforms into amorphous phases. These phase transformations indicate that high-temperature conditions provide a favorable environment for the formation of amorphous Na–Al–Si structures, which enhance aluminum recovery during the alkaline roasting process.

### 3.3. Water leaching

The experimental parameters for roasting temperature, milling time, and BPR determined by the RSM-generated experimental design are presented in Table 3. The aluminum recovery results obtained after milling, roasting, and water leaching under these conditions are also provided in Table 3. The water leaching experiments were conducted under the conditions reported by Sun et al. [5], where the leaching temperature was 75 °C, particle size was -212 µm, leaching time was 15 minutes, and the solution-to-ore ratio was 15:1. For a clearer interpretation of the results, the variation in Al recovery as a function of roasting temperature and milling time is illustrated in the three-dimensional plot presented in Figure 9.

**Table 3.** Aluminum recovery values depending on different milling conditions and roasting temperatures

| Roasting Temperature, °C | Milling time, min. | Ball to ore ratio | %Al recovery |
|---|---|---|---|
| 800 | 113 | 14 | 68.29 |
| 900 | 180 | 20 | 87.93 |
| 800 | 113 | 14 | 67.81 |
| 700 | 180 | 8 | 64.37 |
| 700 | 45 | 20 | 64.65 |
| 900 | 45 | 8 | 84.74 |
| 900 | 45 | 20 | 87.57 |
| 700 | 180 | 20 | 64.41 |
| 800 | 113 | 14 | 67.41 |
| 900 | 180 | 8 | 85.57 |
| 700 | 45 | 8 | 63.10 |
| 800 | 113 | 14 | 66.91 |
| 800 | 113 | 5 | 65.58 |
| 800 | 220 | 14 | 66.06 |
| 963 | 113 | 14 | 87.53 |
| 637 | 113 | 14 | 62.62 |
| 800 | 113 | 14 | 66.57 |
| 800 | 113 | 14 | 66.91 |
| 800 | 2.3 | 14 | 67.22 |
| 800 | 113 | 23 | 68.12 |

In the roasted and intensively milled ore, the dissolved aluminum is considered to originate predominantly from diaspore-derived phases. Increasing the roasting temperature enhances reaction kinetics and thermodynamically favors the formation of water-soluble sodium aluminate ($NaAlO_2$). A pronounced improvement in Al recovery is observed particularly at temperatures of 900 °C and above. This behavior can be attributed to the beneficial effect of high-temperature conditions on both phase transformation and the dissolution kinetics of Al-bearing phases formed during roasting (e.g., $NaAlSiO_4$). In contrast, within the intermediate temperature range (700–800 °C), prolonging the reaction time results in only marginal improvements in recovery, indicating that temperature exerts a more dominant influence than time under these conditions.

Regarding the effect of milling, the limited contribution of extended milling time is likely associated with particle agglomeration, which reduces milling efficiency and restricts further particle-size reduction. Although the average particle size after conventional grinding was 39 µm, it decreased to approximately 10 µm after 45 and 113 min of intensive milling, with similar values obtained for both durations. This substantial decrease in particle size increases the specific surface area and may enhance the dissolution kinetics of Al-bearing phases. Therefore, the observed improvement in Al dissolution efficiency can be partly attributed to surface area enhancement resulting from particle-size reduction. Similar findings have been reported in the literature, where reduced particle size and increased surface area due to milling were shown to improve Al leaching efficiency [27].

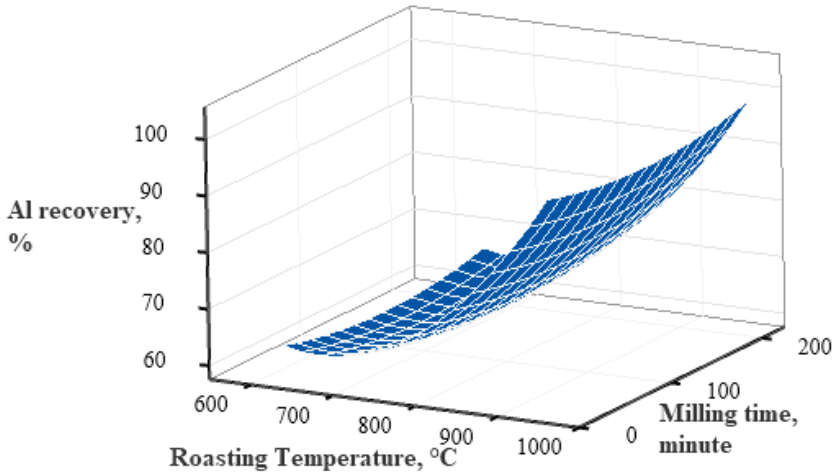


**Figure 9.** Al recovery values as a function of roasting temperature and milling time (Hold value: BPR: 15)

### 3.4. Leaching optimization

The objective of the optimization is to achieve the maximum Al recovery corresponding to the optimum milling conditions and roasting temperature. The model summary statistics related to Al recovery as a function of roasting temperature and milling time are presented in Table 4. The predicted second-order polynomial model equation proposed by the software for the Al recovery response is given in Eq. 3. This equation can be used to make predictions, allowing comparison between the experimental results and the model estimates.

**Table 4.** Summary statistics of the model

| S | R-sq | R-sq(adj) |
|---|---|---|
| 3.64 | 91.99% | 84.78% |

In Table 4, the coefficient of determination ($R^2$) for the second-order regression equation was calculated as 91.99%. The closeness of these values to one another and to 1 indicates the robustness of the model. Furthermore, the $R^2$ and adjusted $R^2$ values exhibit good agreement, demonstrating a high level of model fit. In addition to RSM, an ANOVA was conducted to determine whether there were significant differences among the factor means. The ANOVA results are presented in Table 5. The contour plot is presented in Figure 10.

**Al recovery, %**: $270.8-0.58*A-0.04*B-1.24*C+0.0004*A^2+0.0002*B^2+ 0.03*C^2 + 0.000003*A*B + 0.0008*A*C-0.0006*B*C$ (3)

**Table 5.** ANOVA results showing the effects of different milling conditions and roasting temperature

| Source | DF | Adj SS | Adj MS | F-Value | P-Value |
|---|---|---|---|---|---|
| Model | 9 | 1522.35 | 169.15 | 12.76 | 0.000 |
| Linear | 3 | 1272.32 | 424.11 | 31.98 | 0.000 |
| Roasting Temp. | 1 | 1263.33 | 1263.33 | **95.27** | **0.000** |
| Milling time, min | 1 | 0.00 | 0.00 | 0.00 | 0.990 |
| Ball to ore ratio | 1 | 8.98 | 8.98 | 0.68 | 0.430 |
| Square | 3 | 244.57 | 81.52 | 6.15 | 0.012 |
| Roasting Temp. * Roasting Temp. | 1 | 230.34 | 230.34 | **17.37** | **0.002** |
| Milling time, min * Milling time, min | 1 | 13.57 | 13.57 | 1.02 | 0.336 |
| BPR * BPR | 1 | 15.78 | 15.78 | 1.19 | 0.301 |
| 2-Way Interaction | 3 | 2.11 | 0.70 | 0.05 | 0.983 |
| Roasting Temp. * Milling time, min | 1 | 0.00 | 0.00 | 0.00 | 0.988 |
| Roasting Temp. * BPR | 1 | 1.61 | 1.61 | 0.12 | 0.734 |
| Milling time, min * BPR | 1 | 0.49 | 0.49 | 0.04 | 0.851 |

| | | | | | |
|---|---|---|---|---|---|
| Error | 10 | 132.61 | 13.26 | - | - |
| Lack-of-Fit | 5 | 130.52 | 26.10 | 62.46 | 0.000 |
| Pure Error | 5 | 2.09 | 0.42 | - | - |
| Total | 19 | 1654.96 | - | - | - |

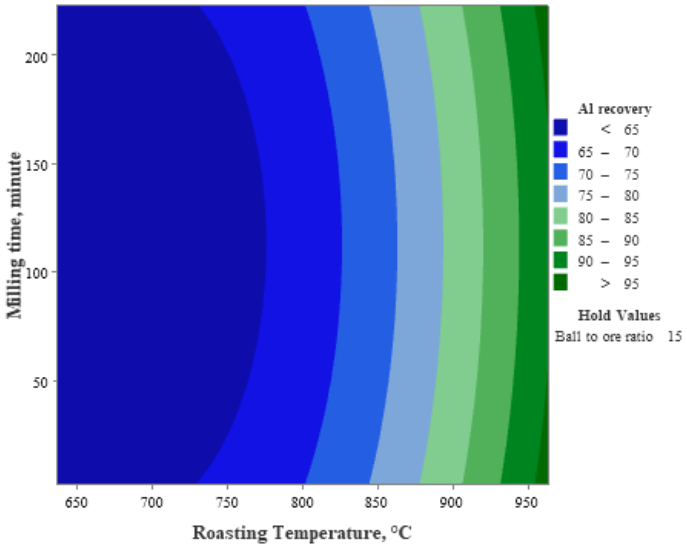


**Figure 10.** Contour plot curves

The most important criteria to consider in the ANOVA table are the F-value and the P-value. A larger F-value indicates a more influential factor. The F-statistic should be interpreted in conjunction with the P-value when determining the significance of the overall results. The P-value, which is derived from the F-statistic, represents the probability that the observed results occurred by chance. For a factor to have a significant effect on the response, its P-value must be less than 0.05 [28-29]. P-values greater than 0.05 indicate that the parameter is insignificant or has no effect on the response. Additionally, it was determined that the roasting temperature is a highly influential factor, whereas the effects of the milling parameters are relatively weak.

According to the contour plot, regions of high Al recovery are represented by green tones. The contour lines indicate that roasting temperature is the determining factor for Al recovery, with a dramatic increase observed at temperatures above 900 °C. The effect of milling time is limited, supporting recovery only in the high-temperature region. The model indicates that the optimum recovery region occurs at a roasting temperature of 900-950 °C and a milling time of 90-200 minutes. To determine the precise optimum parameters, the model was further optimized. The graphs obtained from the RSM optimization are presented in Figure 11.

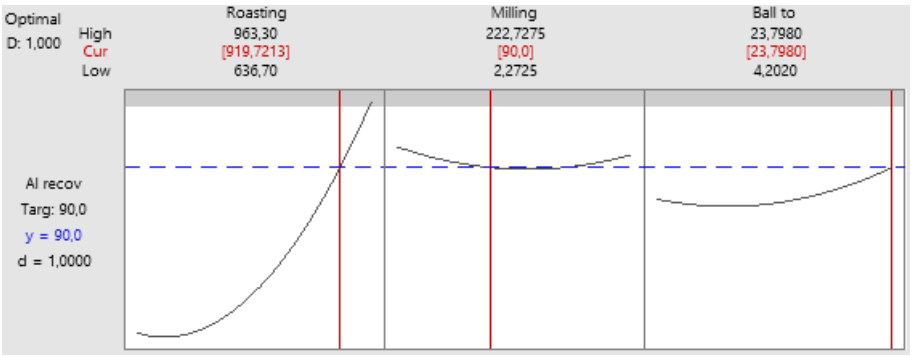


**Figure 11.** Optimum operating conditions and corresponding responses

In Figure 11, the optimum roasting temperature is 919.72 °C, indicating a strong and nonlinear positive effect of temperature on Al recovery. As the roasting temperature increases, Al recovery rises sharply, with the curve

exhibiting a steep upward trend. The optimum milling time is 90 minutes, showing a parabolic trend; recovery decreases at both very short and very long milling durations, with an optimum occurring at an intermediate value. This suggests that prolonged milling can have adverse effects, such as agglomeration and crust formation. The optimum ball-to-ore ratio is 23.8, displaying a slightly sloped parabolic relationship, where medium-to-high values provide optimal recovery. As a result of RSM optimization, a high roasting temperature, intermediate milling time, and medium-to-high BPR collectively provide maximum Al recovery.

High-temperature roasting followed by subsequent leaching processes are known to exhibit thermodynamic trends comparable to those observed in industrial Bayer and sinter processes in terms of aluminum phase transformations and dissolution behavior [9]. Furthermore, findings indicating that mechanical activation enhances Al extraction are consistent with both pilot-scale and industrial studies [27; 30]. This suggests that the results obtained at the laboratory scale hold potential for translation into industrial applications in terms of process optimization.

From an environmental perspective, energy consumption and waste generation are key determining parameters in alumina production processes. Although high-temperature treatments increase energy demand, mechanical activation enhances reaction efficiency, improves recovery rates, and has the potential to reduce the amount of waste generated per unit of product [14]. In addition, achieving higher dissolution efficiency at lower temperatures through mechanical activation may represent an approach capable of reducing the overall energy requirement of the process [10]. In this context, when energy consumption, waste minimization, and resource efficiency are considered collectively, the proposed approach can be regarded as offering potential environmental benefits. However, comprehensive assessments such as life cycle assessment (LCA) and techno-economic analyses are required to clearly quantify these potential gains.

## 4. Conclusions

In this study, the Karaman–Kemiklitepe bauxite ore was characterized and found to contain primarily diaspore, hematite, quartz, albite, and rutile. The ore exhibits an average composition of 47.8% $Al_2O_3$ and 15.6% $SiO_2$, and its high silica content renders it unsuitable for processing via the conventional Bayer method. Therefore, an alkaline roasting–water leaching approach was employed for aluminum extraction. Optimization of the process parameters was conducted using RSM. Regression analyses indicated that the $R^2$ values exceeded 90% for all responses, and the adjusted $R^2$ values were in strong agreement, confirming the robustness and reliability of the developed models in representing the relationships between process variables and responses.The optimized conditions were determined to be a roasting temperature of 919 °C, a milling time of 90 minutes, and a BPR of 23. Among these parameters, roasting temperature was identified as the most influential factor, followed by milling time, whereas the BPR exhibited the least effect.

Water leaching experiments demonstrated that alkaline roasting significantly enhanced aluminum dissolution. Compared with the raw ore, the ore roasted at 1000 °C recovered approximately 26% higher Al recovery. Overall, the findings confirm that the alkaline roasting–water leaching process is an effective and viable method for the treatment of high-silica bauxite ores. This approach offers a promising alternative for the efficient utilization of bauxite resources that cannot be processed by the Bayer method due to their elevated silica content.

## Thanks

The authors thank the GÜBAP2904 Mining Specialization Support Program for financially supporting this study via Project No 24.F5118.04.02. T.U. conceived the study, performed the experiments, interpreted the results, and wrote the manuscript.

## References

[1] Jiang Y, Li W, Feng R. Preparation and performance of 4-alkyl-4,4-bis(hydroxycarbamoyl) carboxylic acid for flotation separation of diaspore against aluminosilicates. Miner Eng 2011; 24: 1571–1579.

[2] Gibson B, Wonyen DG, Chelgani SC. A review of pretreatment of diasporic bauxite ores by flotation separation. Miner Eng 2017; 114: 64–73.

[3] Wu Y, Pan XL, Han YJ, Yu HY. Dissolution kinetics and removal mechanism of kaolinite in diasporic bauxite in alkali solution at atmospheric pressure. Trans Nonferrous Met Soc China 2019; 29: 2627-2637.

[4] Liu W, Yang J, Xiao B. Review on treatment and utilization of bauxite residues in China. Int J Miner Process 2009; 93: 220–231.

[5] Sun Y, Pan A, Ma Y, Chang J. Extraction of alumina and silica from high-silica bauxite by sintering with sodium carbonate followed by two-step leaching with water and sulfuric acid. RSC Adv 2023; 13: 23254.

[6] Valeev D, Shoppert A, Dogadkin D, Romashova T, Kuz'mina T, Salazar-Concha S. Extraction of Al and rare earth elements via high-pressure leaching of boehmite–kaolinite bauxite using $NH_4HSO_4$ and $H_2SO_4$. Hydrometallurgy 2023; 215: 105994.
[7] Ozbag I, Togacar İ, Cinarli Yavas U, Baygül M, Turan A. Alumina extraction from diasporic bauxite via sodium carbonate-assisted roasting and water leaching. Mining Metall Explor 2025; 42:4061–4084.
[8] Li Y, Pan X, Lv Z, Wu H, Yu H. Multi-element comprehensive utilization of high-silicon bauxite by roasting pretreatment and two-stage leaching. Miner Eng 2022; 187: 107805.
[9] Habashi F. Handbook of Extractive Metallurgy, Vol. 2. Heidelberg, Germany: Wiley-VCH, 1997.
[10] Barry TS, Uysal T, Erdemoğlu M, Birinci M. Thermal and mechanical activation in acid leaching processes of non-bauxite ores available for alumina production – Review. Mining Metall Explor 2019; 36: 557–569.
[11] Erdemoğlu M, Birinci M, Uysal T. Alumina production from clay minerals: current review. J Polytechnic 2018; 21(2): 387–396.
[12] Erdemoğlu M, Birinci M, Uysal T. Thermal behavior of pyrophyllite ore during calcination for thermal activation for aluminum extraction by acid leaching. Clays Clay Miner 2020; 68(2): 89–99.
[13] Aydoğmuş R, Erdemoğlu M, Uysal T. Aluminum recovery by acid leaching of variously enriched pyrophyllite ore: effects of pre-treatment methods for activation. Mining Metall Explor 2023; 40: 1333–1343.
[14] Baláž P, Achimovičová M. Mechano-chemical leaching in hydrometallurgy of complex sulphides. Hydrometallurgy 2006; 84: 60–68.
[15] Boldyrev VV. Mechanochemistry and mechanical activation of solids. Solid State Ionics 1993; 63-65: 537–543.
[16] Warris CJ, McCormick PG. Mechanochemical processing of refractory pyrite. Miner Eng 1997; 10: 1119-1125.
[17] Baláž P, Achimovičová M, Billik P, Cherkezova-Zheleva Z, Criado HM, Delogu F, Dutková E, Gaffet E, Gotor FJ, Kumar R, Mitov I, Rojac T, Senna M, Streletskii A, Wieczorek-Ciurowa K. Hallmarks of mechanochemistry: from nanoparticles to technology. Chem Soc Rev 2013; 42: 7571-7637.
[18] Tkáčová K, Baláž P, Mišura B, Vigdergauz VE, Chanturiya VA. Selective leaching of zinc from mechanically activated complex Cu–Pb–Zn concentrate. Hydrometallurgy 1993; 33: 291–300.
[19] Tromans D, Meech JA. Enhanced dissolution of minerals: microtopography and mechanical activation. Miner Eng 1999; 12: 609–625.
[20] Welham NJ. Enhanced dissolution of tantalite/columbite following milling. Int J Miner Process 2001; 61: 145–154.
[21] Pourghahramani P, Forssberg E. Effects of mechanical activation on the reduction behavior of hematite concentrate. Int J Miner Process 2007; 82: 96–105.
[22] Erdemoğlu M, Birinci M, Uysal T. Thermal behavior of pyrophyllite ore during calcination for thermal activation for aluminum extraction by acid leaching. Clays Clay Miner 2020; 68(2): 89–99.
[23] Birinci M, Uysal T, Erdemoğlu M, Porgalı E, Barry T. Acidic leaching of thermally activated pyrophyllite ore from Puturge (Malatya-Turkey) deposit. Proc XVII Balkan Mineral Processing Congress; 1-3 November 2017; Antalya, Türkiye.
[24] Uysal T, Erdemoğlu M, Birinci M. Investigation of activation conditions in alumina production from pyrophyllite ore via acid leaching method. Sci Mining J 2019; 58(2): 111–120.
[25] Uysal T, Erdemoğlu M. Production of aluminum titanate from pyrophyllite ore. J Polytechnic 2021; 25(1): 313–319.
[26] Li Y, Gao Y, Wang X, Shen X, Kong Q, Yu R, Lu G, Wang Z, Chen L. Iron migration and oxygen oxidation during sodium extraction from $NaFeO_2$. Nano Energy 2018; 47: 519–526.
[27] Xue, Y., Zhang, M., Zhou, J., & Zhang, Y. Efficient Al recovery from aluminum dross with simultaneous AlN separation by a mechanical method. Waste 2023; 1(1): 40–51.
[28] Uysal T. Optimization of shape factor by the response surface method, and the effect on sphalerite flotation recovery. J South Afr Inst Min Metall 2023; 123(9): 445–450.
[29] Uysal T, Erust CÜ, Akça ME, Sis H, Erdemoğlu M. Optimization of rare earth elements recovery from Kızıldağ (Karaman–Türkiye) shale ore using response surface methodology. Physicochem Probl Miner Process 2025; 61(3): 205436.
[30] Baláž P. Mechanochemistry in nanoscience and minerals engineering. Berlin, Germany: Springer, 2008.